

STABILITY ANALYSIS OF STRATIFIED LIQUID-LIQUID FLOW

N. BRAUNER and D. MOALEM MARON

Department of Fluid Mechanics and Heat Transfer, Faculty of Engineering, University of Tel-Aviv,
Ramat-Aviv 69978, Tel-Aviv, Israel

(Received 8 February 1990; in revised form 29 July 1991)

Abstract—Linear stability analysis is being widely used in exploring gas–liquid stratified/non-stratified transitions. As the present study relates to *liquid–liquid* two-phase systems, the stability characteristics of stratified layers are considered. In parallel, the conditions necessary for real characteristics are also explored. The relations between stability conditions and those for well-posedness are discussed in view of the implications for flow pattern transitions. The convergence of the stability conditions to various extremes is discussed. The integrated considerations of stability and well-posedness shed light on the physical sequences in flow pattern transitions, which so far have been studied by stability analysis alone. As *liquid–liquid* systems are involved, wide ranges of density and viscosity ratios are studied for various operational conditions.

Key Words: liquid–liquid, stratified two-phase flow, stability, well-posedness, flow pattern transitions

INTRODUCTION

The majority of the extensive literature on two-phase flows refers to gas–liquid systems. Indeed, the intensive research activities regarding a variety of aspects of gas–liquid flows have contributed to a wide understanding. However, there have been relatively very few studies which focused on liquid–liquid two-phase flows. As gas–liquid studies cannot readily be translated to liquid–liquid flow predictions, there is generally an inadequate understanding of the mechanisms and interactions of liquid–liquid systems.

The authors attempted recently to model various two-phase liquid–liquid flow patterns, such as stratified flow (Brauner & Moalem Maron 1989), annular flow (Brauner 1991) and highly viscous core flow (Moalem Maron *et al.* 1990). Of particular interest is the existence of transitional boundaries of these and others possible flow patterns.

In exploring the transitional criteria, one of the basic approaches which may shed light on the range of existence of a specific flow configuration is undoubtedly a stability analysis. For this reason, the use of this approach in gas–liquid studies has become more frequent (Wallis 1969; Jones & Prosperetti 1985; Lin & Hanratty 1986; Prosperetti & Jones 1987). However, gas–liquid systems represent only one extreme with low density and viscosity ratios, both of which play central roles in approaching instability.

Thus, in its first dimension, the present work aims to analyse stability conditions for the wide ranges of density, viscosity and velocity ratios encompassed in liquid–liquid systems. Stratified flow is addressed, since it is considered to be one of the basic flow configurations, which is bounded with other possible flow patterns. The second aspect, dealt with herein, is the development of the conditions under which the set of the governing equations constitutes a well-posed initial-value system, whereby real characteristics are obtained. Clearly, the range where the conditions for well-posedness coincide with those for stability is of particular interest from the point of view of the existence and transition of flow patterns.

The two-fluid uniform velocity approach (depth-averaged equations) is used, as is commonly adopted in numerous gas–liquid studies (Lyczkowski 1978; Ardron 1980; Banerjee & Chan 1980; Banerjee 1985; Hancox *et al.* 1980). The simplified two-fluid uniform velocity formulation facilitates a rather convenient and efficient analysis of both instability and ill-posedness in a pipe geometry with the inclusion of the various shear stress terms. The relations between stability and well-posedness may provide some insight on the relation between the stability of the interfacial structure and transitions to other flow configurations (Brauner & Moalem Maron 1992).

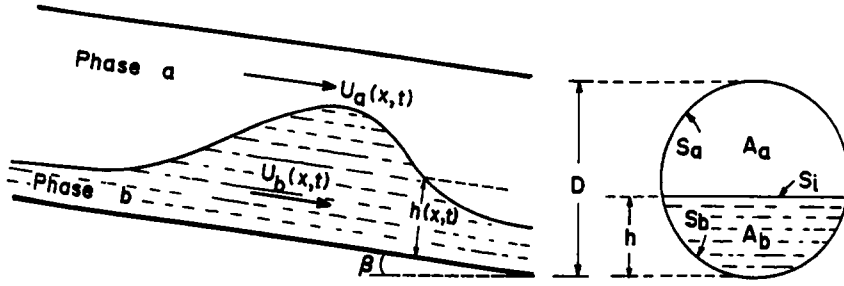


Figure 1. Schematic description of a stratified configuration.

THE PHYSICAL SYSTEM

Consider a stratified flow of two immiscible fluids *a* and *b* in a horizontal (or slightly inclined) conduit. The flow configuration and coordinates are as described in figure 1. Clearly, under the conditions of stratified flow, the lighter fluid forms the upper layer. As the analysis aims to explore the stability features of this flow pattern, the transient continuity and momentum equations for the two fluids are addressed. With reference to figure 1, the two-fluid one-dimensional integral equations are

$$\frac{\partial}{\partial t} (\rho_b A_b) + \frac{\partial}{\partial x} (\rho_b A_b u_b) = 0, \quad [1]$$

$$\frac{\partial}{\partial t} (\rho_a A_a) + \frac{\partial}{\partial x} (\rho_a A_a u_a) = 0, \quad [2]$$

$$\frac{\partial}{\partial t} (\rho_b A_b u_b) + \frac{\partial}{\partial x} (\rho_b A_b \gamma_b u_b^2) = -\tau_b S_b \pm \tau_i S_i + \rho_b A_b g \sin \beta - \frac{\partial}{\partial x} (A_b P_b) + P_{ib} \frac{\partial A_b}{\partial x}, \quad [3]$$

and

$$\frac{\partial}{\partial t} (\rho_a A_a u_a) + \frac{\partial}{\partial x} (\rho_a A_a \gamma_a u_a^2) = -\tau_a S_a \mp \tau_i S_i + \rho_a A_a g \sin \beta - \frac{\partial}{\partial x} (A_a P_a) + P_{ia} \frac{\partial A_a}{\partial x}, \quad [4]$$

where the upper sign in [3] and [4] corresponds to phase *a* faster than *b*. The variables *A*, *S*, τ and *u* are the flow cross section, the wetted perimeter, the wall shear stress and the average velocity of the two fluids, τ_i is the interfacial shear stress. The shape factors, γ_a and γ_b are defined in terms of the local velocity profiles, $u'_{a,b}$:

$$\gamma_a = \frac{1}{A_a u_a^2} \int_0^{A_a} u_a'^2 dA_a; \quad \gamma_b = \frac{1}{A_b u_b^2} \int_0^{A_b} u_b'^2 dA_b. \quad [5]$$

The pressure at each phase varies due to gravity, hence the average pressures P_a and P_b differ from the corresponding values at the common interface, P_{ia} and P_{ib} . The latter may be different due to surface tension effects. The average pressure at each phase, in terms of its pressure level at the free interface, $y = h$, is given by

$$\frac{\partial}{\partial x} (P_b A_b) = \frac{\partial}{\partial x} \int_0^{A_b} [P_{ib} + \rho_b g \cos \beta (h - y)] dA_b = \frac{\partial}{\partial x} (P_{ib} A_b) + \rho_b g \cos \beta A_b \frac{\partial h}{\partial x} \quad [6a]$$

and

$$\frac{\partial}{\partial x} (P_a A_a) = \frac{\partial}{\partial x} \int_0^{A_a} [P_{ia} - \rho_a g \cos \beta (y - h)] dA_a = \frac{\partial}{\partial x} (P_{ia} A_a) + \rho_a g \cos \beta A_a \frac{\partial h}{\partial x}. \quad [6b]$$

Substituting [6] into [3] and [4], while utilizing [1] and [2], respectively, to eliminate the terms $\partial/\partial t(\rho A)_{a,b}$ and subtracting, the resulting combined momentum equations for the two-phases read:

$$\left[\rho_b(1 - \gamma_b) \frac{u_b}{A_b} + \rho_a(1 - \gamma_a) \frac{u_a}{A_a} \right] \frac{dA_b}{dh} \frac{\partial h}{\partial t} + (\rho_b - \rho_a)g \cos \beta \frac{\partial h}{\partial x} + \frac{(\partial P_{ib} - \partial P_{ia})}{\partial x} + \rho_b \frac{\partial u_b}{\partial t} + \rho_b \gamma_b u_b \frac{\partial u_b}{\partial x} - \rho_a \frac{\partial u_a}{\partial t} - \rho_a \gamma_a u_a \frac{\partial u_a}{\partial x} = \Delta f_{ab} \quad [7]$$

and

$$\Delta f_{ab} = -\tau_b \frac{S_b}{A_b} \pm \tau_1 S_1 \left(\frac{1}{A_b} + \frac{1}{A_a} \right) + \tau_a \frac{S_a}{A_a} + (\rho_b - \rho_a)g \sin \beta. \quad [8]$$

The effect of surface tension, σ , is now incorporated in [7] by assuming $P_{ia} \neq P_{ib}$, the difference in which is given by

$$\frac{\partial}{\partial x} (P_{ib} - P_{ia}) = -\frac{\partial}{\partial x} \sigma \frac{\partial^2 h}{\partial x^2} \left[1 + \left(\frac{\partial h}{\partial x} \right)^2 \right]^{3/2}. \quad [9]$$

It is worth pointing out at this stage that [7]–[9] with the continuity equations [1] and [2] constitute a general frame of formulation, except the r.h.s. of the momentum equation, Δf_{ab} . The term Δf_{ab} includes shear stresses, which are to be modelled in terms of the flow variables h , u_a and u_b , according to the particular physical situation under consideration. As most previous works have addressed gas–liquid stratified flows, where $\rho_a \ll \rho_b$, $\mu_a \ll \mu_b$ and $u_a \gg u_b$, the term Δf_{ab} has attained a rather specific modelling. In contrast to the gas–liquid case, the liquid–liquid systems studied herein cover the whole range of density and viscosity ratios, whereby the velocities of two phases may be of comparable levels and the velocity of one phase may exceed that of the other. Therefore, an approach of “adjustable definitions” for the hydraulic diameters of the two fluids, depending on the relative velocity, has been introduced by the authors for liquid–liquid analyses (Brauner & Moalem Maron 1989). According to this approach, the interface is considered as a solid with respect to the fast phase and as a free surface with respect to the slower phase. Detailed modelling of Δf_{ab} in terms of h , u_a and u_b is described in the appendix. For the sake of generality, the analysis proceeds herein in terms of $\Delta f_{ab} = \Delta f_{ab}(h, u_a, u_b)$.

STABILITY ANALYSIS

In order to proceed with the analysis towards the instability and transitional criteria, [1], [2] and [7]–[9] are first linearized around a smooth fully-developed stratified flow pattern (H, U_a, U_b), whereby:

$$h = H + h^*; \quad u_a = U_a + u_a^*; \quad u_b = U_b + u_b^*; \quad \Delta F_{ab}(H, U_a, U_b) = 0. \quad [10]$$

Here, H, U_a, U_b and ΔF_{ab} are obtained by solving the fully-developed stratified flow for a given set of input flow rates of the two fluids involved, as presented elsewhere (Brauner & Moalem Maron 1989). Based on [10], with $h^*/H, u_a^*/U_a, u_b^*/U_b \ll 1$, the linearized forms of [1], [2] and [7] are

$$\left(\mathbf{T} \frac{\partial}{\partial t} + \mathbf{X} \frac{\partial}{\partial x} \right) \boldsymbol{\eta} = \mathbf{F} \boldsymbol{\eta}, \quad [11a]$$

where

$$\mathbf{T} = \begin{bmatrix} A'_b & 0 & 0 \\ -A'_b & 0 & 0 \\ N & \rho_b & -\rho_a \end{bmatrix}, \quad \mathbf{X} = \begin{bmatrix} A'_b U_b & A_b & 0 \\ -A'_b U_a & 0 & A_a \\ G & \rho_b \gamma_b U_b & -\rho_a \gamma_a U_a \end{bmatrix},$$

$$\mathbf{F} = \begin{pmatrix} 0 & 0 & 0 \\ 0 & 0 & 0 \\ \frac{\partial \Delta F_{ab}}{\partial H} & \frac{\partial \Delta F_{ab}}{\partial U_b} & \frac{\partial \Delta F_{ab}}{\partial U_a} \end{pmatrix}, \quad \boldsymbol{\eta} = \begin{pmatrix} h^* \\ u_b^* \\ u_a^* \end{pmatrix};$$

$$G = (\rho_b - \rho_a)g \cos \beta - \sigma \frac{\partial^2}{\partial x^2}; \quad N = \left[\rho_b(1 - \gamma_b) \frac{U_b}{A_b} + \rho_a(1 - \gamma_a) \frac{U_a}{A_a} \right] A'_b;$$

$$A'_b = \left(\frac{dA_b}{dh} \right) \Big|_{(h=H)}; \quad \frac{\partial \Delta F_{ab}}{\partial H} = \frac{\partial \Delta f_{ab}}{\partial h} \Big|_{h=H}; \quad \frac{\partial \Delta F_{ab}}{\partial U} = \frac{\partial \Delta f_{ab}}{\partial u} \Big|_{u=U}. \quad [11b]$$

It is worth noting that \mathbf{T} and \mathbf{X} include the coefficients (of time and space derivatives) evaluated at the fully-developed point (A_a, A_b at $h = H$). Similarly, \mathbf{F} represent the derivatives of ΔF_{ab} with respect to H, U_a and U_b , as detailed in the appendix. Note also that the shape factors relate to the fully-developed profiles, and their time and space variations for small perturbations are of minor consequence.

In order to investigate the stability of [11a], far away from the boundary $x = 0$, the usual temporal formulation is followed:

$$h^* = \hat{h} e^{i(kx - \omega t)}; \quad u_a^* = \hat{u}_a e^{i(kx - \omega t)}; \quad u_b^* = \hat{u}_b e^{i(kx - \omega t)}, \quad [12]$$

where k is a real wave number, $\omega = Ck$ is a complex angular velocity and \hat{h}, \hat{u}_a and \hat{u}_b are (complex) amplitudes of the perturbations. Introducing [12] into [11a] yields

$$\mathbf{M} \hat{\boldsymbol{\eta}} = 0; \quad \hat{\boldsymbol{\eta}} = (\hat{h}, \hat{u}_b, \hat{u}_a)^T, \quad [13]$$

where

$$\mathbf{M} = \begin{pmatrix} \frac{A'_b}{A_b} \left(-\frac{\omega}{k} + U_b \right) & 1 & 0 \\ \frac{A'_b}{A_a} \left(\frac{\omega}{k} - U_a \right) & 0 & 1 \\ -\frac{N\omega}{k} + (\rho_b - \rho_a)g \cos \beta + \sigma k^2 + \frac{i}{k} \frac{\partial \Delta F_{ab}}{\partial H} & -\rho_b \frac{\omega}{k} + \rho_b \gamma_b U_b + \frac{i}{k} \frac{\partial F_{ab}}{\partial U_b} & \rho_a \frac{\omega}{k} - \rho_a \gamma_a U_a + \frac{i}{k} \frac{\partial \Delta F_{ab}}{\partial U_a} \end{pmatrix}.$$

A non-trivial solution exists under the conditions $\det \mathbf{M} = 0$, whereby the dispersion equation is obtained:

$$aC^2 - 2(b_1 + ib_2)C + d_1 + id_2 = 0; \quad C \equiv \omega/k \quad [14a]$$

and

$$C_{1,2} = \frac{1}{a} (b_1 + ib_2) \pm \frac{1}{a} [(b_1 + ib_2)^2 - a(d_1 + id_2)]^{1/2}, \quad [14b]$$

where

$$a = \rho_b \frac{A'_b}{A_b} + \rho_a \frac{A'_b}{A_a},$$

$$b_1 = \rho_b \frac{A'_b}{A_b} \left[1 + \frac{(\gamma_b - 1)}{2} \right] U_b + \rho_a \frac{A'_b}{A_a} \left[1 + \frac{(\gamma_a - 1)}{2} \right] U_a - \frac{1}{2} N,$$

$$b_2 = \frac{1}{2k} \left(\frac{A'_b}{A_b} \frac{\partial \Delta F_{ab}}{\partial U_b} - \frac{A'_b}{A_a} \frac{\partial \Delta F_{ab}}{\partial U_a} \right),$$

$$d_1 = \rho_b \frac{A'_b}{A_b} \gamma_b U_b^2 + \rho_a \frac{A'_b}{A_a} \gamma_a U_a^2 - [(\rho_b - \rho_a)g \cos \beta + \sigma k^2]$$

and

$$d_2 = \frac{1}{k} \left(\frac{A'_b}{A_b} U_b \frac{\partial \Delta F_{ab}}{\partial U_b} - \frac{A'_b}{A_a} U_a \frac{\partial \Delta F_{ab}}{\partial U_a} - \frac{\partial \Delta F_{ab}}{\partial H} \right). \quad [14c]$$

For $k \rightarrow \infty$, both b_2 and d_2 degenerate to zero and

$$C_{1,2} = \frac{b_1}{a} \pm \frac{1}{a} (b_1^2 - ad_1)^{1/2}. \quad [14d]$$

Equations [14a–d] represent the relationship between the (complex) propagation velocity of the disturbance, $C = \omega/k$, to its (real) wave number, k , for a given system geometry and flow operational conditions. The sign of the imaginary part of C determines the stability of the flow, for if there exists any k for which $C_i = \mathcal{I}m[C] > 0$ the stratified flow configuration is unstable (see [12]).

With reference to [14d], for short-wave disturbances, $k \rightarrow \infty$, the quadratic equation [14a] comprises real coefficients, in which case stability is obtained provided the discriminant $b_1^2 - ad_1 \geq 0$, whereby

$$\left(\rho_b \gamma_b \frac{A'_b}{A_b} U_b + \rho_a \gamma_a \frac{A'_b}{A_a} U_a \right)^2 + \left(\rho_b \frac{A'_b}{A_b} + \rho_a \frac{A'_b}{A_a} \right) \times \left[(\Delta \rho g \cos \beta + \sigma k^2) - \rho_b \gamma_b \frac{A'_b}{A_b} U_b^2 - \rho_a \gamma_a \frac{A'_b}{A_a} U_a^2 \right] \geq 0; \quad k \rightarrow \infty. \quad [14e]$$

Equation [14e] for short-wave disturbances is independent of the shear stress modelling, ΔF_{ab} . With the inclusion of surface tension, this condition is always satisfied for sufficiently large k (short waves). However, when surface tension is omitted, an unstable situation may also result for large k . Clearly, the one-dimensional formulation (lateral pressure varies due to hydrostatic effect only) is more valid for long-wave modes.

For $C_r = 0$, the so-called neutral stability conditions are obtained via [14a–c]:

$$C_m = \frac{d_2}{2b_2} = \frac{\frac{A'_b}{A_b} U_b \frac{\partial \Delta F_{ab}}{\partial U_b} - \frac{A'_b}{A_a} U_a \frac{\partial \Delta F_{ab}}{\partial U_a} - \frac{\partial \Delta F_{ab}}{\partial H}}{\frac{A'_b}{A_b} \frac{\partial \Delta F_{ab}}{\partial U_b} - \frac{A'_b}{A_a} \frac{\partial \Delta F_{ab}}{\partial U_a}} \quad [15a]$$

and

$$\left(\rho_b \frac{A'_b}{A_b} + \rho_a \frac{A'_b}{A_a} \right) C_m^2 - 2 \left(\rho_b \gamma_b \frac{A'_b}{A_b} U_b + \rho_a \gamma_a \frac{A'_b}{A_a} U_a \right) C_m + \rho_b \gamma_b \frac{A'_b}{A_b} U_b^2 + \rho_a \gamma_a \frac{A'_b}{A_a} U_a^2 - (\Delta \rho g \cos \beta + \sigma k^2) = 0. \quad [15b]$$

Note that, [15a] represents an explicit expression for the real neutral stable wave velocity, C_m . Inspection of [15a,b] indicates that while [15a] is directly related to the specific modelling of the various shear stresses terms in the two-fluid momentum equations, [15b] is free of the wall and interfacial shear stresses modelling and evolves essentially from the continuity equations and the l.h.s. of the momentum equations. In this sense, the form of [15b] is general and is affected by the modelling of shear stresses only through the C_m value as determined by [15a]. Moreover, [15b] accounts for the velocity distribution (laminar or turbulent) by adjusting appropriate shape factors.

For the sake of physical interpretations and comparison with previous related studies (Wallis 1969; Lin & Hanratty 1986; Hanratty 1987), [15b] is now rearranged in the following form:

$$\frac{\pi^2}{16Dg \cos \beta} \left\{ \frac{\rho_a \tilde{A}'_b}{\rho_b \tilde{A}'_a} U_a^2 \left[\left(\frac{C_m}{U_a} - 1 \right)^2 + (\gamma_a - 1) \left(1 - 2 \frac{C_m}{U_a} \right) \right] + \frac{\tilde{A}'_b}{\tilde{A}'_a} U_b^2 \left[\left(\frac{C_m}{U_b} - 1 \right)^2 + (\gamma_b - 1) \left(1 - 2 \frac{C_m}{U_b} \right) \right] \right\} - \left[\frac{(\rho_b - \rho_a)}{\rho_b} + \frac{\sigma k^2}{\rho_b g \cos \beta} \right] = 0, \quad [15b']$$

with

$$U_{as} = \frac{Q_a}{A}; \quad U_{bs} = \frac{Q_b}{A}; \quad \tilde{A}_{a,b} = \frac{A_{a,b}}{D^2}; \quad \tilde{A}'_b = \frac{d\tilde{A}_b}{d\tilde{H}}; \quad \tilde{H} = \frac{H}{D}. \quad [16]$$

Here, the superficial velocities of the two fluids, U_{as} and U_{bs} , are introduced. In [15b'] gravity (for $\rho_b > \rho_a$) and surface tension terms can be both identified as stabilizing forces. On the other hand, the rest of [15b'] includes the destabilizing effects of the two fluids inertia. For instance, increasing either of the fluid flow rates, may result in an unstable situation.

It is to be emphasized that the disturbance propagation velocity, C_m is generally different from the average velocities of the two fluids, and thus the positive terms of $(C_m/U_a - 1)^2$ and $(C_m/U_b - 1)^2$ are the destabilizing effect. Therefore, while the neglect of C_m/U_a may sometimes be justified in horizontal gas-liquid systems ($U_a \equiv U_G \gg C_m$ and $C_m \simeq U_L$), it is generally unjustified in liquid-liquid systems, where the velocities of the two phases are comparable and the velocity of one phase may exceed that of the other. Also, note that $\gamma_a > 1$ and $\gamma_b > 1$ are destabilizing contributions only for C_m/U_a and $C_m/U_b < 1/2$.

It is further of interest to demonstrate simplifications of [15b'], relevant in some particular physical situations:

- (a) In the extreme of gas-liquid flow, with $U_a \gg C_m$ and $\rho_a \ll \rho_b$, and when turbulent regimes prevail in both the gas and liquid phases ($\gamma_a, \gamma_b \simeq 1$), [15b'] reduces to

$$\frac{\pi^2}{16Dg \cos \beta} \left[\frac{\rho_a \tilde{A}'_b}{\rho_b \tilde{A}_a^3} U_{as}^2 + \frac{\tilde{A}'_b}{\tilde{A}_a^3} U_{bs}^2 \left(\frac{C_m}{U_b} - 1 \right)^2 \right] - \left(\frac{\Delta\rho}{\rho_b} + \frac{\sigma k_n^2}{\rho_b g \cos \beta} \right) = 0. \quad [17]$$

Equation [17] is similar to Lin & Hanratty's (1986) expression, derived for a gas-liquid system (with $\Delta\rho/\rho_b \simeq 1$), except that [17] also includes surface tension effects.

- (b) Further simplification relevant to gas-liquid flows can be obtained when the time and space variations of the (lower) liquid velocity are ignored, whereby [1] and the l.h.s. of [3] both degenerate, implying that a quasi-steady-state is assumed for the lower fluid. Clearly, [13] reduces to a two-dimensional form with respect to (\hat{h}, \hat{u}_a) , which for a non-trivial solution yields

$$C^2 + \left(-2U_a + \frac{i}{\rho_a k} \frac{\partial \Delta F_{ab}}{\partial U_a} \right) C + U_a^2 - \frac{A_a}{A'_b} \left(\frac{\Delta\rho}{\rho_a} g \cos \beta + \frac{\sigma}{\rho_a} k^2 \right) - \frac{i}{\rho_a k} \left(\frac{A_a}{A'_b} \frac{\partial \Delta F_{ab}}{\partial H} + U_a \frac{\partial \Delta F_{ab}}{\partial U_a} \right) = 0. \quad [18]$$

The conditions for neutral stability, by [18], now read:

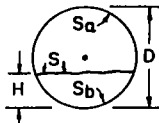
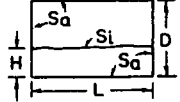
$$U_{as}^2 \left(\frac{C_m}{U_a} - 1 \right)^2 = \frac{16 D \tilde{A}_a^3}{\pi^2 \rho_a \tilde{A}'_b} (\Delta\rho g \cos \beta + \sigma k_n^2) \quad [19a]$$

and

$$C_m = \frac{\left(\frac{A_a}{A'_b} \frac{\partial \Delta F_{ab}}{\partial H} + U_a \frac{\partial \Delta F_{ab}}{\partial U_a} \right)}{\frac{\partial \Delta F_{ab}}{\partial U_a}}. \quad [19b]$$

Equation [19a], for $C_m \ll U_a$ (as is usual in a horizontal gas-liquid system), is similar to the criterion obtained by simply applying Bernoulli's equation in the gas phase with a stationary interfacial disturbance ($C_m \equiv U_b$, otherwise unknown). However, the present analysis includes C_m/U_a in [19a], while [19b] provides the C_m/U_a value in terms of the flow conditions. Note that when $C_m = U_b$ and $\gamma_{a,b} = 1$ are introduced into the general stability condition, [15b'], [19a] with $C_m = U_b$ results.

Table 1 Non-dimensional geometrical variables

	Circular pipe	Rectangular channel
		
$\bar{A} = A/D^2$	$\pi/4$	$L/D = \bar{L}$
$\bar{A}_a = A_a/D^2$	$\frac{1}{4}\{\cos^{-1}(2\bar{H} - 1) - (2\bar{H} - 1)[1 - (2\bar{H} - 1)^2]^{1/2}\}$	$(1 - \bar{H})\bar{L}$
$\bar{A}_b = A_b/D^2$	$\frac{1}{4}\{\pi - \cos^{-1}(2\bar{H} - 1) + (2\bar{H} - 1)[1 - (2\bar{H} - 1)^2]^{1/2}\}$	$\bar{H}\bar{L}$
$\bar{S}_a = S_a/D$	$\cos^{-1}(2\bar{H} - 1)$	$2(1 - \bar{H}) + \bar{L}$
$\bar{S}_b = S_b/D$	$\pi - \cos^{-1}(2\bar{H} - 1)$	$2\bar{H} + \bar{L}$
$\bar{S}_i = S_i/D$	$[1 - (2\bar{H} - 1)^2]^{1/2}$	\bar{L}
$\bar{U}_a = \bar{A}/\bar{A}_a$	$\pi/\{\cos^{-1}(2\bar{H} - 1) - (2\bar{H} - 1)[1 - (2\bar{H} - 1)^2]^{1/2}\}$	$1/(1 - \bar{H})$
$\bar{U}_b = \bar{A}/\bar{A}_b$	$\pi/\{\pi - \cos^{-1}(2\bar{H} - 1) + (2\bar{H} - 1)[1 - (2\bar{H} - 1)^2]^{1/2}\}$	$1/\bar{H}$
$\bar{S}'_b = d\bar{S}_b/d\bar{H}$	$1/[\bar{H}^{1/2}(1 - \bar{H})^{1/2}]$	2
$\bar{S}'_a = d\bar{S}_a/d\bar{H}$	$-1/[\bar{H}^{1/2}(1 - \bar{H})^{1/2}]$	-2
$\bar{S}'_i = d\bar{S}_i/d\bar{H}$	$-2(2\bar{H} - 1)/[1 - (2\bar{H} - 1)^2]^{1/2}$	0
$\bar{A}'_b = d\bar{A}_b/d\bar{H}$	$[1 - (2\bar{H} - 1)^2]^{1/2}$	\bar{L}

(c) In liquid-liquid systems, the lower fluid is sometimes much faster and an extreme situation, similar to case (b), results. Such an extreme situation may be of practical relevance, for example, in the transportation of a waxy oil-water system. Ignoring now the time and space variations in the upper fluid velocity yields, for the neutral stability conditions,

$$U_{bs}^2 \left(\frac{C_m}{U_b} - 1 \right)^2 = \frac{16 D \bar{A}_b^3}{\pi^2 \rho_b \bar{A}_b'} (\Delta \rho g \cos \beta + \sigma k^2) \quad [20a]$$

and

$$C_m = \frac{\left(U_b \frac{\partial \Delta F_{ab}}{\partial U_b} - \frac{A_b}{A_b'} \frac{\partial \Delta F_{ab}}{\partial H} \right)}{\frac{\partial \Delta F_{ab}}{\partial U_b}} \quad [20b]$$

(d) For stratified flow between horizontal parallel plates, where, $A_b = \bar{H}D$, $A_b' = 1$ and $A_a = (1 - \bar{H})D$ (see table 1), the equivalent of [15b] reads

$$\frac{1}{Dg \cos \beta} \left\{ \frac{U_{bs}^2}{\bar{H}^3} \left[\left(\frac{C_m}{U_b} - 1 \right)^2 + (\gamma_b - 1) \left(1 - 2 \frac{C_m}{U_b} \right) \right] + \frac{\rho_a}{\rho_b} \frac{U_a^2}{(1 - \bar{H})^3} \right. \\ \left. \times \left[\left(\frac{C_m}{U_a} - 1 \right)^2 + (\gamma_a - 1) \left(1 - 2 \frac{C_m}{U_a} \right) \right] \right\} - \left(\frac{\rho_b - \rho_a}{\rho_b} + \frac{\sigma k_n^2}{\rho_b g \cos \beta} \right) = 0, \quad [21]$$

which is again in close similarity to the expression obtained by Hanratty (1987).

It is to be noted that maintaining both continuity equations [1] and [2], while assuming quasi-steady momentum equations for either of the two fluids (as when referring to kinematic waves), again yields the simplified equations [18]–[20], as in cases (b) and (c). On the other hand, retaining $\partial/\partial x$ while ignoring $\partial/\partial t$ in the momentum equation of the faster fluid does not simplify the resulting dispersion equation relative to the general case of [14a–d]. [The term $(1 - C_m/U_a)^2$ in [15b'] is then replaced by $(1 - C_m/U_a)$ if $U_a \gg U_b$, or $(1 - C_m/U_b)^2$ is replaced by $(1 - C_m/U_b)$ if $U_b \gg U_a$.]

CONDITIONS FOR REAL CHARACTERISTICS

The continuity equations [1] and [2] with the combined momentum equation [7] constitute the governing set of transient equations. The initial-value (hyperbolic) equations set is well-posed,

provided it possesses real characteristics. As the test for reality of characteristics is carried out around an initially fully-developed stratified flow pattern (at $t = 0$), [11a] is used as the working set, whereby the characteristic roots, λ , are obtained by

$$\det(\mathbf{T} - \lambda \mathbf{X}) = 0. \quad [22]$$

As the well-posedness test will be carried out below in relation to the growth of harmonic interfacial disturbances, $\sigma \partial^3 h / \partial x^3 = -\sigma k^2 \partial h / \partial x$; whereby [22] reads

$$\left(\rho_b \frac{A'_b}{A_b} + \rho_a \frac{A'_a}{A_a} \right) \lambda^2 - 2 \left(\rho_b \gamma_b \frac{A'_b}{A_b} U_b + \rho_a \gamma_a \frac{A'_b}{A_a} U_a \right) \lambda + \rho_b \gamma_b \frac{A'_b}{A_b} U_b^2 + \rho_a \gamma_a \frac{A'_b}{A_a} U_a^2 - (\Delta \rho g \cos \beta + \sigma k^2) = 0. \quad [23]$$

The condition for real characteristics is now obtained from [23] by avoiding any complex root for λ . Thus,

$$\left(\rho_b \gamma_b \frac{A'_b}{A_b} U_b + \rho_a \gamma_a \frac{A'_b}{A_a} U_a \right)^2 - \left(\rho_b \frac{A'_b}{A_b} + \rho_a \frac{A'_b}{A_a} \right) \times \left[-(\Delta \rho g \cos \beta + \sigma k^2) + \rho_b \gamma_b \frac{A'_b}{A_b} U_b^2 + \rho_a \gamma_a \frac{A'_b}{A_a} U_a^2 \right] \geq 0 \quad [24a]$$

or

$$\frac{D}{\rho_{ab}} (\Delta \rho g \cos \beta + \sigma k^2) + \tilde{\rho}_b \gamma_b (\gamma_b - 1) U_b^2 + \tilde{\rho}_a \gamma_a (\gamma_a - 1) U_a^2 - (\gamma_b U_b - \gamma_a U_a)^2 \geq 0, \quad [24b]$$

where

$$\tilde{\rho}_b = 1 + \frac{\rho_b \tilde{A}_a}{\rho_a \tilde{A}_b}; \quad \tilde{\rho}_a = 1 + \frac{\rho_a \tilde{A}_b}{\rho_b \tilde{A}_a}; \quad \rho_{ab} = \frac{\tilde{A}_b}{\tilde{A}_a \tilde{A}_b} \frac{\rho_a \rho_b}{\frac{\tilde{A}_a}{\rho_a} + \frac{\tilde{A}_b}{\rho_b}} = \frac{\rho_a \tilde{A}_b}{\tilde{\rho}_a \tilde{A}_a}. \quad [25]$$

Inspection of [24b] points out that for the case of zero gravity and zero surface tension terms, the basic continuity and momentum equations for plug flow ($\gamma_a = \gamma_b = 1$) are obviously ill-posed, as demonstrated by Ramshaw & Trapp (1978) for inviscid systems and $\gamma_a = \gamma_b = 1$. However, since the general solution of [22] and [23], as well as [24a,b], is independent of the viscous shear terms (r.h.s. of momentum equations, Δf_{ab} in [7]), the assumption of inviscid fluids has no effect. The inclusion of either gravity or surface tension, is thus, necessary for obtaining real characteristics in two-fluid plug flow, $\gamma_a = \gamma_b = 1$. However, for shape factors $\gamma_a, \gamma_b > 1$, well-posedness may still be obtained in the absence of gravity and surface tension forces. Stated differently, a velocity distribution is a stabilizing contribution.

Some specific physical situations are demonstrated now in view of [24a,b]:

(a) For turbulent flow regimes in both phases, when $\gamma_a = \gamma_b \simeq 1$, [24a,b] become

$$(U_b - U_a)^2 \leq \frac{D}{\rho_{ab}} (\Delta \rho g \cos \beta + \sigma k^2); \quad [26]$$

which for particular system of horizontal gas-liquid flow, when $U_a \gg U_b$ and $A_a/\rho_a \gg A_b/\rho_b$, reduces to

$$U_{as}^2 \leq \frac{16}{\pi^2} \frac{1}{\rho_a} \frac{D \tilde{A}_a^3}{\tilde{A}_b} (\Delta \rho g \cos \beta + \sigma k^2). \quad [27]$$

It is noteworthy, however, that it is necessary that both $U_a \gg U_b$ and $A_a/\rho_a \gg A_b/\rho_b$ hold for [27] to be a valid approximation. This may not always be the case, e.g. at relatively low gas-liquid flow rates ratios, in which case [24a,b] or [26] are to be used.

- (b) Another specific system of interest may be the flow between horizontal parallel plates (spaced a distance D apart) for which [24a,b] and [25] for $\gamma_a = \gamma_b = 1$ simplify to

$$(U_a - U_b)^2 \leq \frac{D}{\rho_{ab}} (\Delta\rho g \cos \beta + \sigma k^2) \quad [28a]$$

with

$$\rho_{ab} = \frac{1}{\frac{\tilde{H}}{\rho_b} + \frac{(1-\tilde{H})}{\rho_a}}; \quad \tilde{H} = \frac{H}{D}. \quad [28b]$$

RELATIONSHIPS BETWEEN STABILITY AND REALITY OF CHARACTERISTICS

It is commonly believed that a correct mathematical presentation of physical situations ought to result in properly posed problems. In two-phase flow problems, however, the existence of an assumed physical situation, e.g. a stratified flow configuration, is not certain under all operational conditions. Therefore, complex characteristics (improperly posed initial-value problem) may not necessarily indicate an incorrect formulation, but may be attributed to a physical instability of the assumed flow configuration, whereby transition to a different flow pattern may take place. It is thus the purpose of the present discussion to show the overlap and distinction between the conditions derived herein for stability and reality of characteristics.

The first comparison of interest is that between [14e] and [24a]. Inspection of [14e] and [24a] indicates that in the limit of very short waves, $k \rightarrow \infty$, the condition for stability of smooth stratified flow, [14e], and that for reality of characteristics, [24a], become completely identical, whereby $b_1^2 - ad_1 \geq 0$ is required. It is noted that in the presence of finite surface tension and with $k \rightarrow \infty$, [14e] and [24a] are trivially satisfied, independently of the specific operational conditions. For zero surface tension, however, either of the above two conditions define a range of operational conditions (U_{as}, U_{bs}), where both stability and well-posedness are assured for $k \rightarrow \infty$.

Another comparison of interest is the particular case of gas-liquid flow, where usually $C_m/U_a \rightarrow 0$ is assumed, and the stability condition given by [19a] and the corresponding one developed for real characteristics, [27], are again identical, independently of the disturbance wavelength. Clearly, for the symmetrical case of a much faster lower phase, $C_m/U_b \rightarrow 0$, the regions for stability and reality of characteristics coincide again for the entire range of wave numbers.

More general relations between stability and well-posedness can be derived by comparing [15b] and [23]. Both evolve from the l.h.s. of the continuity and momentum equations and are thus common to any one-dimensional stratified two-fluid model, independently of the specific (quasi-steady) modelling of the interfacial and wall shear stresses (r.h.s. of the momentum equation). Note, however, that [15b] is subject to [15a], which in turn relates directly to the shear stresses modelling. Equation [15b] for neutral stable conditions, as evolved from stability analysis, and [23] for the characteristic roots, are both quadratic with completely identical coefficients. Therefore, the existence of real characteristics for which the discriminant of [23] is positive (hence the discriminant for [15b] as well) corresponds to real solution for $\lambda = C_m$. Yet, this alone does not ensure a (neutral) stable situation, since the real C_m obtained in this way does not necessarily fulfil [15a]. This is best explained with reference to figure 2.

Figure 2 represents typical trends of the amplification factor, $C_i = \mathcal{I}_m\{C\}$ with the wave number, in terms of (U_{as}, U_{bs}) combinations, as obtained by [14a-d] for an oil-water system. For a certain set of (U_{as}, U_{bs}), as depicted by curves (a), there exists no wave number for which the amplification is positive. Thus, for the entire range of k (or wavelengths), all disturbances are expected to decay. On the other hand, for other combinations of (U_{as}, U_{bs}), as in curves (c), a smooth (stable) interfacial structure is maintained for $k > k_n$. For $0 < k < k_n$, or sufficiently long waves, where the destabilizing effect of surface tension becomes small, the disturbances are amplified and hence a wavy interfacial structure develops. The range of amplified waves, $0 < k < k_n$, varies depending on the (U_{as}, U_{bs}) combinations. For particular combinations of (U_{as}, U_{bs}), as represented by curves (b),

the amplified range almost diminishes. In searching for all combinations of (U_{as}, U_{bs}) for which $k_n \rightarrow 0$, a boundary which confines all possible smooth stratified flows, "zero neutral stability" (ZNS) boundary, may be defined (Brauner & Moalem Maron 1992).

For each combination of (U_{as}, U_{bs}) the range for amplified wave numbers is directly obtained by solving [15] for k_n . For the same (U_{as}, U_{bs}) conditions, [24a] is also solved for $k = k_{rc}$ beyond which ($k > k_{rc}$) the characteristic roots are real. For comparison the minimum wave number which ensures real characteristics, k_{rc} , is also indicated in figure 2. For all $k < k_{rc}$, an unstable smooth stratified flow is consistently predicted by both stability and well-posedness analyses. However, for any $k_{rc} < k < k_n$, while the governing equations [1]-[3] are well-posed as an initial-value problem, they are still expected to develop a wavy structure.

It is to be emphasized that the value of k_{rc} is always within the amplified range, $k_{rc} < k_n$, as shown in figure 2. This can be rigorously understood in view of [23] and [15b]. With the minimum $k (\equiv k_{rc})$ which renders a positive discriminant for [23], and therefore also for [15b], the C_m value obtained by [15b] does not necessarily fulfil [15a]. In order to obtain the "true" C_m of [15a], which certainly ought to be real, a larger $k (=k_n \geq k_{rc})$ is required. Thus, as long as [24] yields a real k_{rc} it

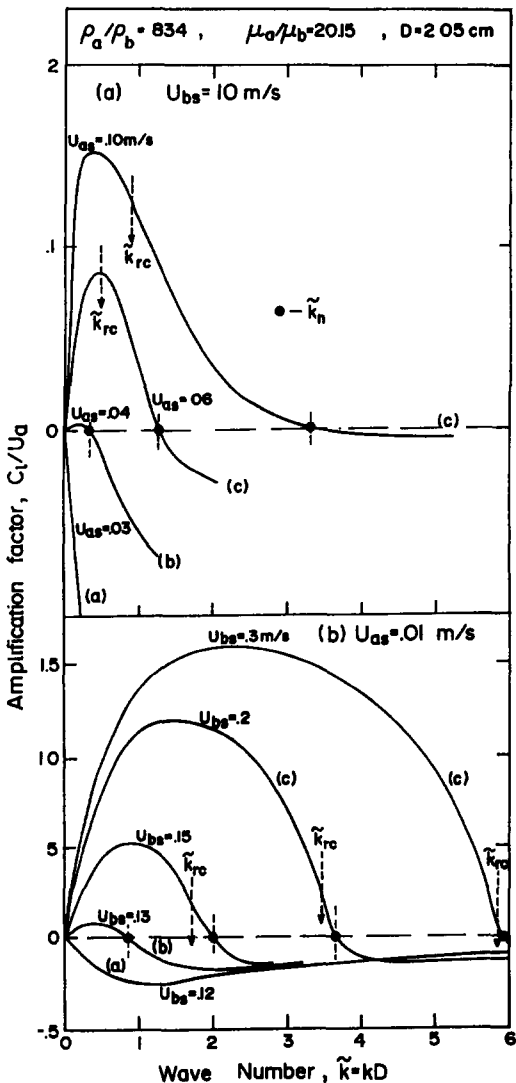


Figure 2. Amplification factor for various oil and water flow rates.

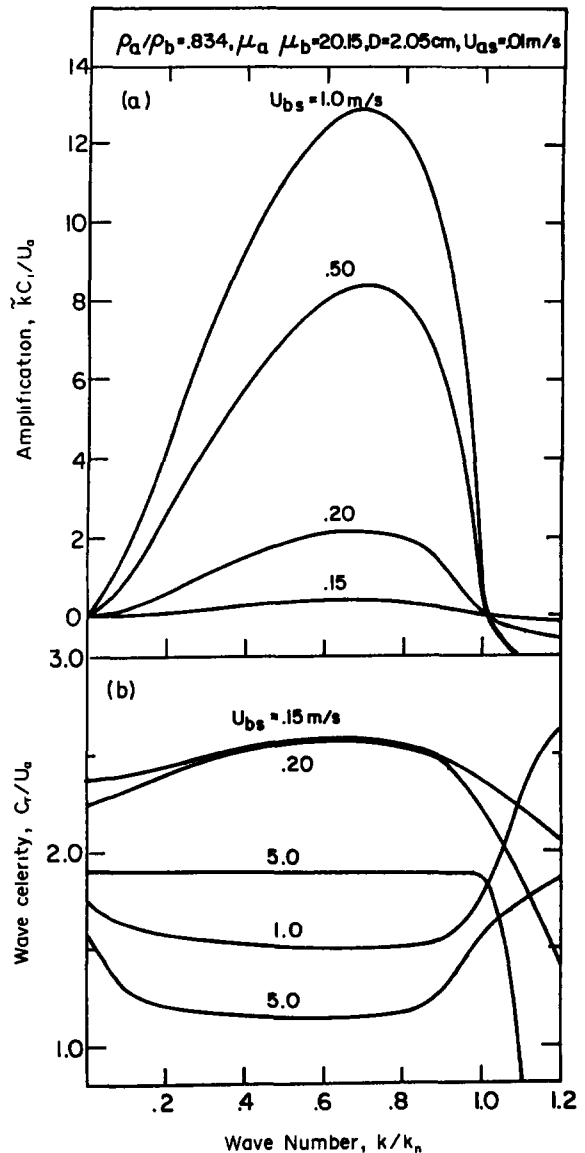


Figure 3. Wave amplification and celerity vs non-dimensional wave number.

corresponds to an amplified mode. The first interpretation for this outcome is that reality of characteristics is a necessary condition for stability, but clearly not sufficient. Similarly to the ZNS boundary (defined for $k_n \rightarrow 0$), the limiting operational condition (U_{as}, U_{bs}), which yields real characteristics for $k_{rc} \rightarrow 0$, defines the “zero real characteristics” (ZRC) boundary. The implications of the ZRC and ZNS boundaries with regard to transition from smooth stratified flow is discussed in detail elsewhere (Brauner & Moalem Maron 1992).

Figure 3 represents the variation of the dimensionless amplification, $\tilde{\omega}_i = kDC_i/U_a$ and wave celerity, C_r/U_a with the normalized wave number, k/k_n . In general, the amplification demonstrates a maximum for $k < k_n$, which corresponds to the most amplified wave number, $k = k_m$. The corresponding wave celerity at $k = k_m$ (for a given U_{bs}) may be higher, equal or lower than the wave celerity of the neutral stable wave, $k = k_n$, as demonstrated in figure 3(b). Note that figure 3 relates to oil-water flow, for which the lower layer b is always faster than the upper layer ($U_b > U_a$). As is shown in figure 3(b), the wave velocity at the amplified region, $0 \leq k/k_n \leq 1$, is of the order of the upper lower layer velocity U_a .

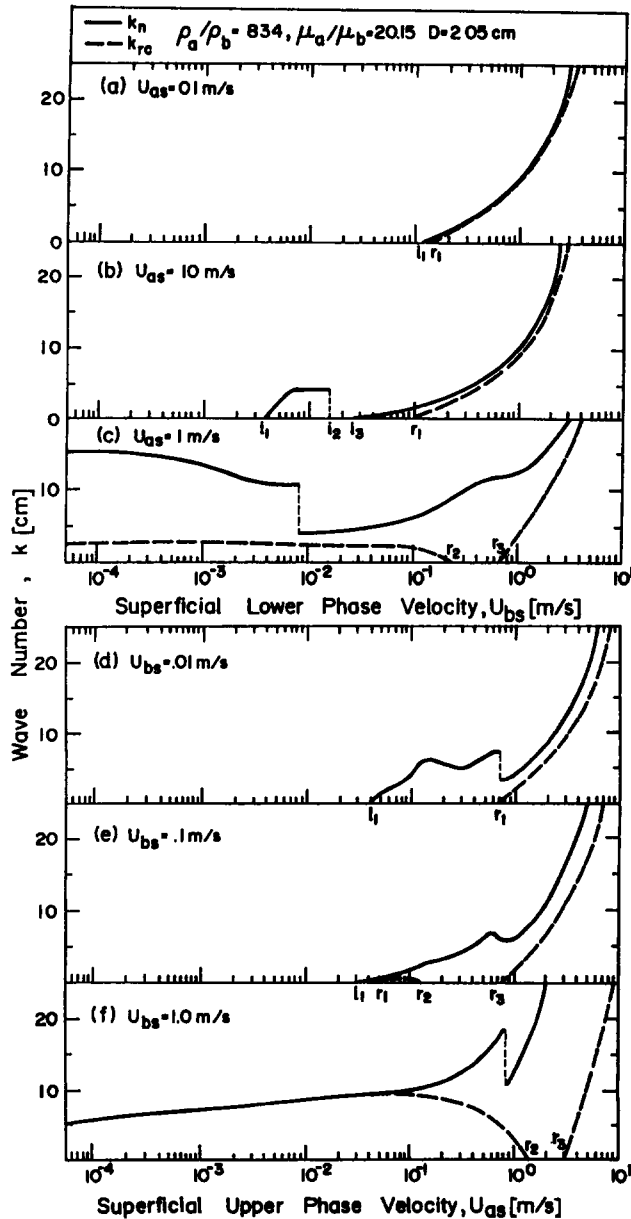


Figure 4. Neutral stable wave number and minimal wave number for obtaining real characteristics for various oil and water rates.

Complementary to figures 2 and 3 is figure 4, where the neutral stable wave number, k_n and the minimum wave number for real characteristics k_{rc} , are compared. Consistent with figure 2, k_{rc} is always lower than k_n for all flow situations. Thus, for flow conditions below those of points i_1 , at which $k_n = 0$, no real solution for k_n is obtained by [15b], implying a stable stratified flow. Similarly, the points denoted by r_1 , at which $k_{rc} = 0$, represent the limiting conditions below which real characteristics are always ensured, while beyond points r_1 reality of characteristics is ensured only for wave numbers higher than k_{rc} . As is indicated in figure 4, the trends of both k_n and k_{rc} with increasing phase flow rates are not always monotonous. In general, the discontinuities in the k_n curves [as in figure 4(b) at point i_2] are due to flow regime transitions of one of the phases. Moreover, for particular U_{as} or U_{bs} multiple solutions for $k_n = 0$ or $k_{rc} = 0$ may be obtained. For instance, between i_2 and i_3 and r_2 and r_3 stable subregions result in addition to the stable region below i_1 and r_1 . On the other hand, for sufficiently high flow rates [figure 4(c,f)] $k_n > 0$ always, hence smooth stratified flow is unstable for $0 < k < k_n$. The k_{rc} subregions between r_2 and r_3 at high flow rates can be best understood in view of [26]. Between r_2 and r_3 , U_a and U_b become close and for a finite gravity term, [26] does not yield a real solution for k_{rc} . It is worth noting here that the reality of characteristics, in general, is directly related to the velocity difference between the phases, whereas the stability condition is sensitive to the ratio between the interfacial wave velocity and the phase velocity, C_m/U_a or C_m/U_b , see [15b].

The results so far relate to various flow conditions and a particular oil–water system for which $\rho_a/\rho_b = 0.834$ and $\mu_a/\mu_b = 20.15$ [experimental setting by Russell *et al.* (1959)]. As the present work attempts to study a wide range of liquid–liquid systems, the discussion proceeds hereon to demonstrate the effects of density and viscosity on the stability characteristics.

Figures 5 and 6 show the effect of the density on various characteristic wave numbers (k_n , k_m and k_{rc}) and the corresponding wave velocities at various flow conditions. With reference to figure 5,

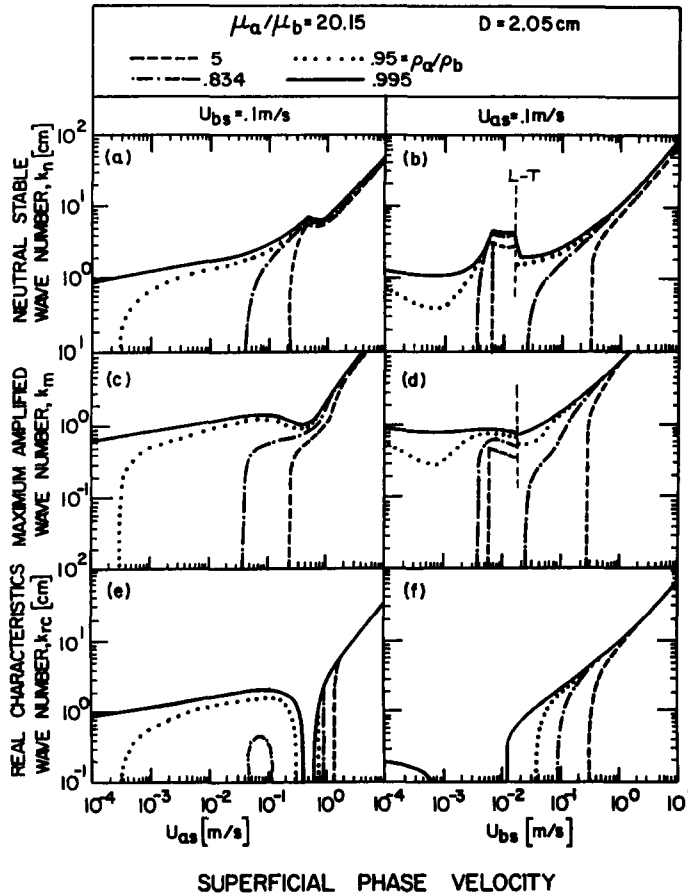


Figure 5. Effects of the density differential and the two fluid flow rates on the characteristic wave numbers k_n , k_m and k_{rc} .

it is seen that with an increasing density differential, both k_n and k_{rc} decrease and thus the range of amplified wave numbers or that for improperly posed problems are both reduced. However, for high U_{as} or U_{bs} the effect of the density ratio is not a dominant one and the k_n range is governed essentially by the flow conditions. Also, with an increasing density differential, the range of flow rates (U_{as} or U_{bs}) for stable smooth stratified flow increases. The maximum amplified wave number, k_m , follows, in general, the k_n trends. The discontinuities [as in figures 5(b,c) and 6(f)] are again due to flow regimes transitions. Note that in the equal velocity zone, $U_a/U_b \approx 1$, k_{rc} may exhibit a limited subzone of U_{as} or U_{bs} where the formulation is well-posed with respect to all wave modes.

In figure 6, the neutral stable and most amplified wave celerities [C_m and C_{m^*} normalized with respect to the slower phase according to figure 6(c,d)] are presented. Inspection of figure 6(a,b) reveals that the celerities are both of the order of the slower layer velocity, for a wide range of the velocity ratio, U_a/U_b . Moreover, the effect of the density ratio on the wave celerity, as well as on the phases velocities ratio is practically negligible for $\rho_a/\rho_b = 0.5$ to 1. Figure 6(c,d) shows that, in contrast to horizontal gas-liquid flows, in liquid-liquid systems the velocities of the two phases may be of comparable levels and the velocity of the upper lighter phase may be lower or higher than that of the other heavier layer.

Some additional information may be derived by referring to the maximum amplification rate, as in figure 6(e,f). The maximum amplification rate (normalized with respect to the slower phase) increases with a decreasing density difference, indicating again more favourable conditions for the evolution of wavy interfacial structure and hence departure from smooth stratified flow.

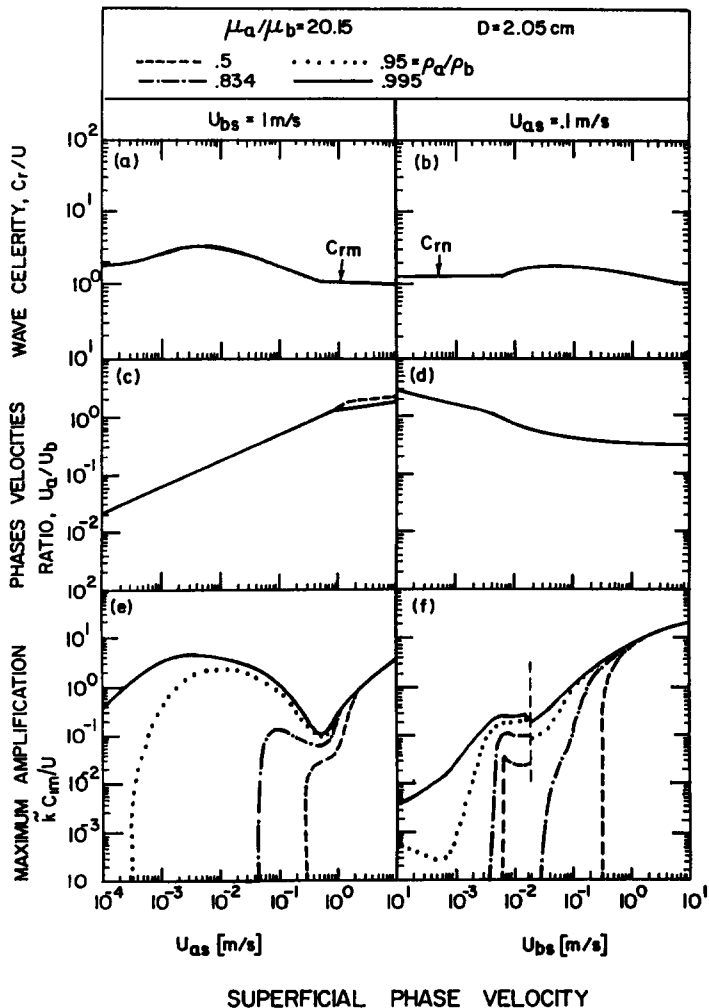


Figure 6. Effects of the density differential and the two fluid flow rates on the wave celerity, the phases velocities ratio and the maximum wave amplification.

In parallel to figures 5 and 6 the effects of the viscosity ratio on the instability characteristics are briefly summarized in view of figures 7 and 8. In principle, increasing or decreasing the viscosity ratio ($\mu_a/\mu_b > 1$ or $\mu_a/\mu_b < 1$) is associated with a larger velocity gap between the two layers, due to the larger viscosity differential, $\Delta\mu$, as demonstrated in figure 8(b). Consequently, for a given density ratio and flow rates (U_{as}, U_{bs}), in general, a larger viscosity gap affects flow instability. Indeed, as shown in figure 7, the departure from equal viscosities ($\mu_a/\mu_b \neq 1$), corresponds to increased k_n and k_{rc} , implying a wider range of unstable modes with more intense amplification rates [see figure 8(c)]. However, the instability characteristics are not directly related to the velocity gap and also depend on the other flow variables. For instance, the neutral stable wave number, k_n , relates among others to the non-dimensional wave velocities, C_m/U_a and C_m/U_b (see [15b']). These are presented in figure 8(a), and are shown to vary over a wide range with an increasing viscosity gap. At high viscosity ratios, $\mu_a/\mu_b \gg 1$, the interfacial wave celerity may significantly exceed the slower (viscous) layer velocity ($C_m/U_a \gg 1$).

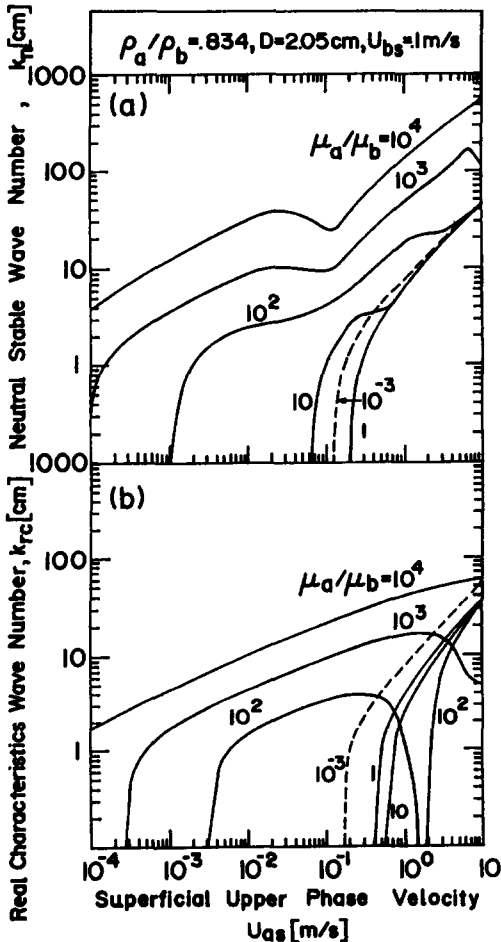


Figure 7. Effect of the viscosity ratio on the characteristic wave numbers k_n and k_{rc} .

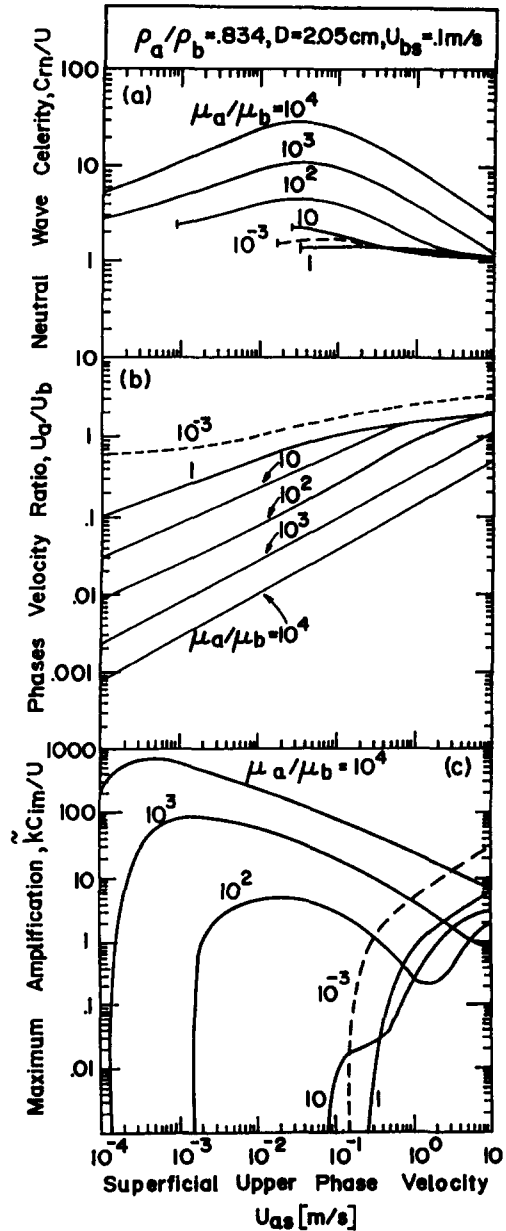


Figure 8. Effect of the viscosity ratio on the phases velocities ratio, neutral stable wave celerity and maximum amplification.

FINAL NOTES

It is of interest to comment further on the instability characteristics of the basic stratified configuration by referring to an alternative spatial instability formulation of the governing equations and its relation to the temporal formulation. Also, the non-dimensional groups which govern the instability conditions are identified and discussed.

Spatial formulation

The temporal formulation [12] has been used by most investigators in order to analyse flow instability. The temporal formulation assumes harmonic disturbances in space (x) which are imposed at a specified time ($t = 0$), and which may grow or decay with time. Clearly, a non-periodic disturbance may be described, in the frame of linear analysis, in terms of periodic modes by the appropriate Fourier series expansion (in x). On the other hand, spatial formulation assumes disturbances which take place at a specified location ($x = x_0$) and are harmonic in time. Again, any non-periodic disturbance in time may be analysed in terms of its (time) Fourier series presentation. In this case the assumed disturbances grow or decay spatially.

In reality, the stratified flow is exposed to random perturbations in space and time, and thus temporal and spatial formulations, though they represent simplification of the physical situations, may provide complementary information. In addition, for some particular problems, the spatial formulation ought to be adopted (as in the analysis of stationary waves or artificially incepted waves by a wave maker). From the mathematical point of view, while the temporal formulation assumes a real wave number and a complex wave frequency (or velocity), in the spatial formulation the frequency is real and the wave number is complex.

Following the spatial formulation, the perturbations in [12] are assumed now to be of real frequency, ω , and complex wave number, k . Introducing [12] into [11a], the condition for the non-trivial solution reads in this case:

$$\sigma k^4 + ak^2 + [2b_1 - ib_2]k - (c_1 + ic_2) = 0, \quad [29a]$$

where

$$\begin{aligned} a &= (\rho_b - \rho_a)g \cos \beta - \rho_b \gamma_b \frac{A'_b}{A_b} U_b^2 - \rho_a \gamma_a \frac{A'_a}{A_a} U_a^2, \\ b_1 &= \left\{ \rho_b \frac{A'_b}{A_b} \left[1 + \frac{(\gamma_b - 1)}{2} \right] U_b + \rho_a \frac{A'_a}{A_a} \left[1 + \frac{(\gamma_a - 1)}{2} \right] U_a - \frac{N}{2} \right\} \omega, \\ b_2 &= \frac{A'_b}{A_b} U_b \frac{\partial F_{ab}}{\partial U_b} - \frac{A'_a}{A_a} U_a \frac{\partial F_{ab}}{\partial U_a} - \frac{\partial F_{ab}}{\partial H} \end{aligned}$$

and

$$c_1 = \left(\rho_b \frac{A'_b}{A_b} + \rho_a \frac{A'_a}{A_a} \right) \omega^2, \quad c_2 = \left(\frac{A'_b}{A_b} \frac{\partial F_{ab}}{\partial U_b} - \frac{A'_a}{A_a} \frac{\partial F_{ab}}{\partial U_a} \right) \omega. \quad [29b]$$

Equation [29a], in contrast to [14a], is a fourth-order algebraic equation for the complex wave number (given a specified ω). It determines the unstable modes; for if $k_i = \mathcal{I}m(k) < 0$, the disturbance of a frequency, ω and a wavelength given by $2\pi/k$, (originated at some specified location) will grow downstream. Note that for zero surface tension, or in the limit of weakly amplified long waves ($|k| \rightarrow 0$), [29a] reduces again to a quadratic equation which yields an explicit expression for k in terms of the frequency:

$$k_{1,2} = \frac{1}{a} \left(b_1 - \frac{ib_2}{2} \right) \pm \frac{1}{a} \left[\left(b_1 - \frac{ib_2}{2} \right)^2 + a(c_1 + ic_2) \right]^{1/2}; \quad \sigma \rightarrow 0 \text{ or } |k| \rightarrow 0. \quad [30]$$

Of particular interest are the conditions for neutral stability, $k_i = \mathcal{I}m(k) = 0$. Utilizing real k in [29a], the requirement for non-complex solutions for $k(\omega)$ leads to two relations identical to [15a,b] as obtained with the temporal formulation. Hence, as long as instability and transition are explored with reference to the neutral stability conditions, the temporal and spatial formulations are *equivalent*. Moreover, for the weakly amplified waves near the neutral stable modes, the spatial (S)

and temporal (T) solutions can be related by the Gaster's (1962) transformation (Brauner *et al.* 1987), whereby

$$k_r(\text{T}) = k_r(\text{S}), \quad \omega_r(\text{T}) = \omega_r(\text{S}), \quad \frac{\omega_r(\text{T})}{k_r(\text{S})} = -\frac{\partial \omega_r}{\partial k_r} = -\frac{\partial(k_r C_g)}{\partial k_r} = -C_g; \quad [31]$$

where C_g is the group velocity. For non-dispersive waves the group velocity equals the phase velocity, C_r . Indeed, as shown in figure 3(b) the amplified modes may demonstrate a weak dispersion, in which case by [31] $C_g \simeq C_r$ and the temporal and spatial amplifications are simply related by the (real) wave celerity.

Non-dimensional groups

Equation [15b'] for neutral stability conditions and [24b] for ensuring well-posedness are, in essence, the governing relations for exploring the instability of the otherwise smooth stratified configuration. The non-dimensional forms of [15b'] and [24b] are:

$$\begin{aligned} \frac{\tilde{A}'_b}{\tilde{A}'_a} \left[\left(\frac{C_m}{U_a} - 1 \right)^2 + (\gamma_a - 1) \left(1 - 2 \frac{C_m}{U_a} \right) \right] \text{Fr}_a^2 \\ + \frac{\tilde{A}'_b}{\tilde{A}'_b} \left[\left(\frac{C_m}{U_n} - 1 \right)^2 + (\gamma_b - 1) \left(1 - 2 \frac{C_m}{U_b} \right) \right] \text{Fr}_b^2 - \frac{16}{\pi^2} (1 + \tilde{k}_n^2 \text{We}_b \text{Fr}_b^2) = 0; \end{aligned} \quad [32a]$$

$$\begin{aligned} \text{Fr}_a^2 = \frac{\rho_a}{\Delta \rho} \frac{U_{as}^2}{Dg \cos \beta}; \quad \text{Fr}_b^2 = \frac{\rho_b}{\Delta \rho} \frac{U_{bs}^2}{Dg \cos \beta} = \frac{\rho_b}{\rho_a} \frac{\text{Fr}_a^2}{\phi^2}; \quad \phi = \frac{U_{as}}{U_{bs}} \\ \tilde{k} = kD; \quad \text{We}_a = \frac{\sigma}{\rho_a D U_{as}^2} = \frac{\rho_b}{\rho_a} \frac{\text{We}_b}{\phi^2}; \end{aligned} \quad [32b]$$

and

$$\frac{\tilde{\rho}_b \gamma_b (\gamma_b - 1)}{\tilde{A}_b^2} + \frac{\rho_a \gamma_a (\gamma_a - 1) \phi^2}{\tilde{A}_a^2} + \frac{16}{\pi^2} (\text{Fr}_{ab}^{-2} + \text{We}_{ab} \tilde{k}_{rc}^2) - \left(\frac{\gamma_b}{\tilde{A}_b} - \frac{\phi \gamma_a}{\tilde{A}_a} \right)^2 = 0; \quad [33a]$$

$$\text{Fr}_{ab}^2 = \frac{\rho_{ab} U_{bs}^2}{\Delta \rho Dg \cos \beta}; \quad \text{We}_{ab} = \frac{\sigma}{D \rho_{ab} U_{bs}^2}; \quad [33b]$$

where Fr_a , Fr_b , Fr_{ab} , We_a , We_{ab} and \tilde{k} represent Froude, Weber and non-dimensional wave numbers, respectively. For $\gamma_a, \gamma_b = 1$, [33a,b] reduce to

$$\frac{\pi^2 \tilde{A}'_b}{16 \tilde{A}_a} \left(\frac{\rho_a \tilde{A}_b}{\rho_b \tilde{A}_a} + 1 \right)^{-1} \left(\frac{1}{\phi \tilde{A}_b} - \frac{1}{\tilde{A}_a} \right)^2 = (\text{Fr}_a^{-2} + \text{We}_a \tilde{k}_{rc}^2). \quad [34]$$

Inspection of [32]–[34] indicates that for a given pair of fluids, the ZNS boundaries, [32a,b] with $k_n = 0$, as well as the ZRC boundary, [33a,b] with $k_{rc} = 0$, are determined by three parameters: χ^2 and ϕ , which are the steady-state parameters (see the appendix), and an additional Froude number (Fr_a or Fr_b) which evolves in the stability analysis. The relationships between the χ^2 and ϕ parameters depend on the fluids physical properties of the fluids and the flow regimes of the phases (Brauner & Moalem Maron 1989). The Weber number, which is relevant for determining the stability characteristics, is irrelevant at the transitional boundaries when derived with reference to $k_n \rightarrow 0$ and $k_{rc} \rightarrow 0$.

Implications for flow pattern transitions

The analyses of stability and well-posedness presented above are aimed at establishing a basis for the construction of the complete transitional boundaries from stratified flow to other bounding patterns in a variety of two-fluid systems. The application of the integrated frame of stability and well-posedness considerations for constructing flow pattern maps is the focus of the companion

paper (Brauner & Moalem Maron 1992). Here, however, some of the relevant outlines are briefly noted.

The stability and well-posedness analyses yield two boundaries of particular interest: the ZNS and ZRC lines as defined in relation to the limit of zero wave number (long waves). These two boundaries constitute a "stability and well-posedness" map. In this map, the region beyond the ZNS line represents the range of operational conditions, for which the interface is associated with the evolution of amplified modes. Beyond the ZRC line, part of the amplified modes are ill-posed. It is shown that while the ZNS line represents a lower bound for the transition from (smooth) stratified flow, the ZRC line relates to an upper bound for the existence of a (wavy) stratified configuration. This implies that the departure from a stratified pattern is not predictable by a single stability criterion but rather in terms of a "buffer" transitional zone, as is formed between the ZNS and the ZRC lines.

The exact relations between the "stability and well-posedness" maps and detailed guidelines for constructing flow pattern maps in liquid-liquid, gas-liquid, horizontal or inclined systems will follow in subsequent studies.

REFERENCES

- ARDON, K. H. 1980 One-dimensional two-fluid equations for horizontal stratified two-phase flow. *Int. J. Multiphase Flow* **6**, 295–305.
- BANERJEE, S. 1985 Multifield modelling of two-phase flow: problems and potential. Presented at the *2nd Int. Conf. on Multiphase Flow*, London.
- BANERJEE, S. & CHAN, A. M. C. 1980 Separated flow modes—I. Analysis of the averaged and local instantaneous formulations. *Int. J. Multiphase Flow* **6**, 1–24.
- BRAUNER, N. 1991 Two-phase liquid-liquid annular flow. *Int. J. Multiphase Flow* **17**, 59–76.
- BRAUNER, N. & MOALEM MARON, D. 1989 Two-phase liquid-liquid stratified flow. *PhysicoChem. Hydrodynam.* **11**, 487–506.
- BRAUNER, N. & MOALEM MARON, D. 1992 Flow pattern transitions in two-phase liquid-liquid flow in horizontal tubes. *Int. J. Multiphase Flow* **18**, 123–140.
- BRAUNER, N., MOALEM MARON, D. & ZIJL, W. 1987 Interfacial collocation equations in thin liquid films: stability analysis. *Chem. Engng Sci.* **42**, 2025–2036.
- GASTER, M. 1962 A note on the relation between temporally-increasing and spatially-increasing disturbances in hydrodynamic stability. *J. Fluid Mech.* **14**, 222–224.
- HANCOX, W. T., FERCH, R. L., LIU, W. S. & NIEMAN, R. E. 1980 One-dimensional models for transient gas-liquid flows in ducts. *Int. J. Multiphase Flow* **6**, 25–40.
- HANRATTY, T. J. 1987 Gas-liquid flow in pipes. *PhysicoChem. Hydrodynam.* **9**, 101–114.
- JONES, A. V. & PROSPERETTI, A. 1985 On the suitability of first-order differential models for two-phase flow prediction. *Int. J. Multiphase Flow* **11**, 133–148.
- LIN, P. Y. & HANRATTY, T. J. 1986 Prediction of the initiation of slugs with linear stability theory. *Int. J. Multiphase Flow* **12**, 79–98.
- LYCZKOWSKI, R. W., GIDASPOW, D., SOLBRIG, C. W. & HUGHES, E. D. 1978 Characteristics and stability analysis of transient one-dimensional two-phase flow equations and their finite difference approximations. *Nucl. Sci. Engng* **66**, 378–396.
- MOALEM MARON, D., BRAUNER, N. & KRUKA, V. 1990 The mechanism of two-phase liquid-liquid core-flow. Presented at the *6th Miami Int. Symp. on Heat and Mass Transfer*, Miami, FL.
- PROSPERETTI, A. & JONES, A. V. 1987 The linear stability of general two-phase flow models. *Int. J. Multiphase Flow* **13**, 161–171.
- RAMSHAW, J. D. & TRAPP, J. A. 1978 Characteristics, stability and short-wavelength phenomena in two-phase flow equation systems. *Nucl. Sci. Engng* **66**, 93–102.
- RUSSELL, T. W. F., HODGSON, G. W. & GOVIER, G. W. 1959 Horizontal pipe line flow of oil and water. *Can. J. Chem. Engng* **27**, 9–17.
- WALLIS, G. B. 1969 *One-dimensional Two-phase Flow*. McGraw-Hill, New York.

APPENDIX

Quasi-steady Modelling of Shear Stress Terms and Their Linearized Forms

The governing combined momentum equation, [7], requires the expressions for τ_a , τ_b and τ , in terms of the velocities of the two fluids. As conventionally used in two-fluid models, the wall shear stresses τ_a and τ_b are expressed in terms of the corresponding friction factors f_a and f_b :

$$\tau_a = f_a \rho_a \frac{u_a^2}{2}; \quad f_a = c_a \left(\frac{D_a u_a}{\nu_a} \right)^{-n_a} = c_a \text{Re}_a^{-n_a}. \quad [\text{A.1a}]$$

and

$$\tau_b = f_b \rho_b \frac{u_b^2}{2}; \quad f_b = c_b \left(\frac{D_b u_b}{\nu_b} \right)^{-n_b} = c_b \text{Re}_b^{-n_b}. \quad [\text{A.1b}]$$

Note that the corresponding Reynolds numbers for the two fluids are based on the equivalent hydraulic diameters, defined according to the relative velocity of the phases:

$$D_a = \frac{4A_a}{(S_a + S_i)}; \quad D_b = \frac{4A_b}{S_b} \quad \text{for } u_a > u_b \quad [\text{A.2a}]$$

$$D_a = \frac{4A_a}{S_a}; \quad D_b = \frac{4A_b}{(S_b + S_i)} \quad \text{for } u_a < u_b \quad [\text{A.2b}]$$

$$D_a = \frac{4A_a}{S_a}; \quad D_b = \frac{4A_b}{S_b} \quad \text{for } u_a \simeq u_b. \quad [\text{A.2c}]$$

In contrast to gas–liquid flows (where the gas velocity is of a higher order of magnitude and therefore the interface is considered as a free surface with respect to the liquid and as a stationary surface with respect to the fast gas phase), in liquid–liquid systems the velocities of the two phases may be of comparable levels and, alternatively, one phase velocity may exceed the other. Therefore, an *adjustable* definition of the equivalent hydraulic diameter as part of the solution procedure needs to be adopted (Brauner & Moalem Maron 1989).

The constants c_a , c_b , n_a and n_b in [A.1] are chosen according to the flow regime in each phase. Clearly, the two phases in stratified flow may result in laminar–laminar (L–L), laminar–turbulent (L–T), turbulent–laminar (T–L) or turbulent–turbulent (T–T) regimes. These constants are given the following values: $c = 16$, $n = 1$ for laminar flow; and $c = 0.046$, $n = 0.2$ for turbulent flow conditions.

In [1], [2] and [8], τ_i stands for the interfacial shear stress between the two layers. A positive τ , corresponds to a faster upper layer or, in general,

$$\tau_i = f_i \frac{\rho (u_a - u_b)^2}{2}, \quad [\text{A.3}]$$

with

$$\rho = \rho_a \quad \text{and} \quad f_i = B f_a \quad \text{for } u_a > u_b$$

$$\rho = \rho_b \quad \text{and} \quad f_i = B f_b \quad \text{for } u_b > u_a.$$

Equations [A.3] imply that the interfacial shear friction factor is evaluated as equal to that obtained between the faster phase and the pipe wall, augmented by a factor B due to interfacial waviness. For $u_a \simeq u_b$, τ_i is identically zero and thus the interface is considered as a free surface with respect to both phases, consistent with [A.2c].

The linearization of [7] requires, furthermore, the linearized forms of the various shear stress terms around the smooth fully-developed stratified flow defined by U_a , U_b and H . Thus, consistent with [A.1]–[A.3], the three members of the matrix \mathbf{F} defined in [11a] are:

$$\frac{\partial F_{ab}}{\partial U_b} = -S_b \frac{\rho_b}{A_b} f_b U_b \left(1 - \frac{n_b}{2} \right) \pm S_i \left(\frac{1}{A_a} + \frac{1}{A_b} \right) \frac{\partial \tau_i}{\partial U_b}, \quad [\text{A.4a}]$$

$$\frac{\partial \tau_i}{\partial U_b} = \begin{cases} -Bf_a \rho_a (U_a - U_b) & U_a > U_b, \\ Bf_b \rho_b (U_b - U_a) \left[1 - \frac{n_b (U_b - U_a)}{2 U_b} \right] & U_a < U_b; \end{cases} \quad \begin{matrix} \text{[A.4b]} \\ \text{[A.4c]} \end{matrix}$$

$$\frac{\partial F_{ab}}{\partial U_a} = S_a \frac{\rho_a}{A_a} f_a U_a \left(1 - \frac{n_a}{2} \right) \pm S_i \left(\frac{1}{A_a} + \frac{1}{A_b} \right) \frac{\partial \tau_i}{\partial U_a}, \quad \text{[A.5a]}$$

$$\frac{\partial \tau_i}{\partial U_a} = \begin{cases} Bf_a \rho_a (U_a - U_b) \left[1 - \frac{n_a (U_a - U_b)}{2 U_a} \right] & U_a > U_b, \\ -Bf_b \rho_b (U_b - U_a) & U_a < U_b; \end{cases} \quad \begin{matrix} \text{[A.5b]} \\ \text{[A.5c]} \end{matrix}$$

and

$$\begin{aligned} \frac{\partial F_{ab}}{\partial H} = & \left[-\tau_b \frac{\partial}{\partial h} \left(\frac{S_b}{A_b} \right) - \frac{1}{2} \left(\frac{S_b}{A_b} \right) \rho_b U_b^2 \frac{\partial f_b}{\partial h} \pm \tau_i \frac{\partial}{\partial h} \left(\frac{S_i}{A_a} + \frac{S_i}{A_b} \right) \right. \\ & \left. \pm \frac{1}{2} S_i \left(\frac{1}{A_a} + \frac{1}{A_b} \right) B \rho (U_a - U_b)^2 \left(\frac{\partial f_i}{\partial h} \right) + \tau_a \frac{\partial}{\partial h} \left(\frac{S_a}{A_a} \right) + \frac{1}{2} \frac{S_a}{A_a} \rho_a U_a^2 \left(\frac{\partial f_a}{\partial h} \right) \right] \Big|_{h=H}, \end{aligned} \quad \text{[A.6a]}$$

$$\frac{\partial f_a}{\partial h} \Big|_{h=H} = \frac{\partial f_a}{\partial H} = \begin{cases} -n_a \frac{f_a}{D} \left(-\frac{\tilde{A}'_b}{\tilde{A}_a} + \frac{\tilde{S}'_b}{\tilde{S}_a} \right) & \frac{U_a}{U_b} \leq r_c \\ -n_a \frac{f_a}{D} \left(-\frac{\tilde{A}'_b}{\tilde{A}_a} - \frac{\tilde{S}'_i - \tilde{S}'_b}{\tilde{S}_i + \tilde{S}_a} \right) & \frac{U_a}{U_b} > r_c, \end{cases} \quad \text{[A.6b]}$$

$$\frac{\partial f_b}{\partial h} \Big|_{h=H} = \frac{\partial f_b}{\partial H} = \begin{cases} -n_b \frac{f_b}{D} \left(-\frac{\tilde{A}'_b}{\tilde{A}_b} - \frac{\tilde{S}'_b}{\tilde{S}_b} \right) & \frac{U_b}{U_a} \leq r_c \\ -n_b \frac{f_b}{D} \left(\frac{\tilde{A}'_b}{\tilde{A}_b} - \frac{\tilde{S}'_i + \tilde{S}'_b}{\tilde{S}_i + \tilde{S}_b} \right) & \frac{U_b}{U_a} > r_c, \end{cases} \quad \text{[A.6c]}$$

$$\frac{\partial f_i}{\partial H} = \frac{\partial f_b}{\partial H}; \quad \rho = \rho_b; \quad U_b > U_a$$

$$\frac{\partial f_i}{\partial H} = \frac{\partial f_a}{\partial H}; \quad \rho = \rho_a; \quad U_b < U_a. \quad \text{[A.6d]}$$

Where r_c is a prescribed velocity ratio for switching from [A.2c] to [A.2a] when $U_a > r_c U_b$, or from [A.2c] to [A.2b] when $U_b > r_c U_a$. Note that the various steady-state flow variables required in the above equations are determined from the steady-state solutions in terms of non-dimensional χ^2 , Y and ϕ parameters defined by (Brauner & Moalem Maron 1989):

$$\phi = \frac{U_{as}}{U_{bs}}; \quad \chi^2 = \frac{\frac{4c_b}{D} \frac{\rho_b U_{bs}^2}{\left(\frac{U_{bs} D}{v_b} \right)^{-n_b} 2}}{\frac{4c_a}{D} \frac{\rho_a U_{as}^2}{\left(\frac{U_{as} D}{v_a} \right)^{-n_a} 2}}; \quad Y = \frac{(\rho_b - \rho_a) g \sin \beta}{\frac{4c_a}{D} \frac{\rho_a U_{as}^2}{\left(\frac{U_{as} D}{v_a} \right)^{-n_a} 2}}. \quad \text{[A.7]}$$